3-29-2109

Light Scattering by Pure Seawater: Effect of Pressure

Lianbo Hu

Xiaodong Zhang
University of North Dakota, xiaodong.zhang2@UND.edu

Mary Jane Perry

Deep-Sea Research Part I 146 (2019) 103–109

Contents lists available at ScienceDirect

Deep-Sea Research Part I

journal homepage: www.elsevier.com/locate/dsri

Light scattering by pure seawater: Effect of pressure

Lianbo Hu[a,b], Xiaodong Zhang[c,*], Mary Jane Perry[d]

[a] Department of Earth System Science and Policy, University of North Dakota, Grand Forks, ND, 58202, USA
[b] Ocean Remote Sensing Institute, Ocean University of China, Qingdao, 266003, Shandong, China
[c] Division of Marine Science, University of Southern Mississippi, Stennis Space Center, MS, 39529, USA
[d] School of Marine Sciences, University of Maine, Orono, ME, 04469, USA

ARTICLE INFO

Keywords:
Light scattering
Seawater
Pressure
Particulate backscattering
Thermodynamics

ABSTRACT

The Zhang et al. model [Optics Express, **17**, 5698-5710 (2009)] for calculating light scattering by seawater does not account for pressure, which should, theoretically, affect molecular scattering. While negligible in near surface waters, the error associated with this approximation could be significant when backscattering is measured directly in the deep ocean, by deep CTD casts or biogeochemical-Argo floats, for example. We updated the parameterization in the Zhang et al. model using (1) the Millard and Seaver equation for the refractive index of seawater [Deep Sea Research Part A, **37**, 1909-1926 (1990)] and (2) the Feistel equation for Gibbs free energy for seawater thermodynamics [Deep-Sea Research I, **55**, 1639-1671 (2008)]. As these equations include the effect of pressure as well as salinity and temperature, our new parameterization allows us to investigate the potential effect of pressure on scattering. Increasing pressure suppresses the random motion of molecules, reducing the fluctuations in both density and concentration, which in turn causes an overall decrease in light scattering by seawater. For pure water and seawater with a salinity of 34 PSU, the decreases are approximately 13% and 12%, respectively, with a 100-MPa (approximately the pressure of seawater at 10000 m) increase in pressure. Below the thermocline and/or halocline where temperature and salinity change slowly, the steady increase of pressure is the dominant factor affecting the light scattering by seawater. At depths where backscattering is typically dominated by molecular scattering by seawater, particulate backscattering would be underestimated if the effect of pressure on molecular scattering were not considered.

1. Introduction

Light scattering by seawater is an inherent optical property of the ocean, and forms background scattering that is unavoidably measured by scattering sensors and must be corrected to derive the particulate scattering. According to the Smoluchowski-Einstein theory (Smoluchowski, 1908; Einstein, 1910), scattering by a macroscopically uniform dense media, such as pure water, is caused by thermal motion-induced microscopic fluctuations in density, which in turn cause microscopic fluctuations in the refractive index. Following this theory, the volume scattering functions due to density fluctuations at a scattering angle of 90°, $\beta_d(90)$, can be modeled as

$$\beta_d(90) = \frac{\pi^2}{2\lambda^4} k_B T \beta_T \left(\rho \frac{\partial n^2}{\partial \rho}\right)^2, \quad (1)$$

where λ is the wavelength of light in vacuum, k_{BB} is the Boltzmann constant, and T, β_T, n, and ρ are the absolute temperature, the isothermal compressibility, the refractive index, and the density of water, respectively.

The presence of dissolved salts in seawater modifies the terms β_T, n, and ρ in Eq. (1), which, in turn, causes a slight decrease in $\beta_d(90)$ with increasing salinity (Zhang et al., 2009). Another impact of the presence of dissolved salts is the microscopic fluctuations in concentration (i.e., the mixing ratio between water molecules and disassociated sea salt ions) that induce additional fluctuations in the refractive index (Einstein, 1910). From thermodynamic statistics, Zhang et al. (2009) derived the scattering due to fluctuations in concentration, $\beta_c(90)$, as a function of salinity, S_A

$$\beta_c(90) = \frac{\pi^2}{2\lambda^4} \frac{M_w}{N_A \rho} \left(\frac{\partial n^2}{\partial S_A}\right)^2 \frac{S_A}{-\partial \ln a_0 / \partial S_A}, \quad (2)$$

where S_A is the absolute salinity in g kg^{-1}, M_w is the molecular weight of water, N_A is Avogadro's number, and a_0 is the activity of water. The absolute salinity, S_A, differs from the Practical Salinity S (PSU) in both its definition and values, where $S_A = 1.0047 \times S$ (Millero et al., 2008). $\beta_c(90)$ increases with salinity at a much greater rate than the slight

* Corresponding author.
E-mail address: xiaodong.zhang@usm.edu (X. Zhang).

https://doi.org/10.1016/j.dsr.2019.03.009
Received 22 January 2019; Received in revised form 20 March 2019; Accepted 24 March 2019
Available online 29 March 2019

decrease of $\beta_d(90)$ (Zhang et al., 2009). Therefore, $\beta_c(90) + \beta_d(90)$, representing the net effect of sea salts on scattering, increases with salinity.

As water molecules are anisotropic, fluctuations in the orientation of water molecules enhance the overall scattering by a Cabannes factor $f(\delta)$ (Cabannes, 1922),

$$f(\delta) = \frac{6 + 6\delta}{6 - 7\delta} \tag{3}$$

where δ is the depolarization ratio of water. The total molecular scattering by seawater ($\beta(90)$) represents the combined effect of fluctuations in density, salt concentrations and molecule orientation,

$$\beta(90) = (\beta_d(90) + \beta_c(90))f(\delta). \tag{4}$$

Using the latest measurements of state and thermodynamic variables, and the depolarization ratio, Zhang and Hu (2009a) and Zhang et al. (2009) demonstrated that the spectral scattering by pure water and seawater can be predicted using Eqs. (1)–(4), agreeing with the measurements by Morel (1966, 1974) with a difference of < 2%. While the scattering by seawater is expected to vary with temperature, salinity, and pressure, the parameterization developed in the models (Zhang and Hu, 2009a; Zhang et al., 2009) for n, β_T, ρ, and a_0 did not consider the effect of pressure (P). Therefore, these models should only be used for near-surface waters, where the changes in pressure with depth are limited. The change in pressure, and its effect, however, is significant when scattering measurements are taken over a range of great depths, by deep CTD casts or biogeochemical-Argo (BGC-Argo) profiling floats, for example. To the best of our knowledge, no studies, theoretical or experimental, have been conducted that investigate the changes in scattering by pure water or seawater in response to pressure. Currently, we do not even know the direction of possible changes. Therefore, the primary motivation of this study is to fill this knowledge gap. One immediate application of this theoretical development is to correct the scattering by seawater from *in situ* measurements of backscattering in deep water.

2. Methodology

To investigate the effect of pressure on light scattering by seawater, the parameterization of the terms involving n, β_T, ρ, and a_0 in Eqs. (1) and (2) needs to be updated by considering pressure. While we still do not know if and how the depolarization ratio of water changes with pressure, we assume a constant value of 0.039, which was measured by Farinato and Rowell (1976) and recommended for use by the ocean optics community (Werdell et al., 2018).

The empirical equation developed by Quan and Fry (1995) (QF) for the refractive index of seawater was used in the models of molecular scattering by pure water (Zhang and Hu, 2009a) and pure seawater (Zhang et al., 2009). While it is valid for $0\,^\circ\mathrm{C} < T < 30\,^\circ\mathrm{C}$, $0‰ < S < 35‰$, and $400\,\mathrm{nm} < \lambda < 700\,\mathrm{nm}$, this refractive index model does not include pressure. The equation for the refractive index of seawater developed by Millard and Seaver (1990) (MS) covers ranges of 500–700 nm, 0–30 °C, 0–40 PSU, and 0–110 MPa for wavelength, temperature, salinity, and pressure, respectively. We examined the performance of the Millard and Seaver (1990) refractive index model for seawater using three high-quality experimental databases (Mehu and Johannin-Gilles, 1968; Stanley, 1971; Daimon and Masumura, 2007) (Fig. 1). Overall, we found that the MS equation agrees with these measurements within their respective experimental errors over its performance range. Compared to the Stanley (1971) measurements of the refractive index of seawater at pressures of 34.5, 68.9, and 103.5 MPa, the MS equation has lower residuals (Δn) than the experimental errors of 6×10^{-5} (Fig. 1(a)). Also, the residuals exhibit no clear covariations with either temperature or wavelength, indicating the residuals are more or less randomly distributed and suggesting that the MS equation does not incur systematic errors in accounting for the effect of pressure on the refractive index of seawater. We found that the MS equation performs better than the QF equation in comparison to the Mehu and Johannin-Gilles (1968) measurements, which were used to develop the QF equation (Fig. 1(b)). However, the residuals of both equations are mostly within the experimental error of 3×10^{-5}. Spectrally, the MS equation agrees with the Daimon and Masumura (2007) measurements, with residuals within their experimental error of 8×10^{-6} for λ in the range of 500–700 nm (Fig. 1(c)). Over a broader spectral range of 400–900 nm, the MS equation performs better than the QF equation, with an uncertainty of $< 4 \times 10^{-5}$. From the evaluation shown in Fig. 1, we decided to use the MS equation for the refractive index of seawater, as it accounts for the effect of pressure and performs better than the QF equation.

Similar to Zhang and Hu (2009a), the $\rho\frac{\partial n^2}{\partial \rho}$ term in Eq. (1) is expressed following Proutiere et al. (1992) as:

$$\rho\frac{\partial n^2}{\partial \rho} = (n^2 - 1)\left[1 + \frac{2}{3}(n^2 + 2)\left(\frac{n^2 - 1}{3n}\right)^2\right]. \tag{5}$$

There is no analytical expression for the $\frac{\partial n^2}{\partial S_A}$ term in Eq. (2); hence, we rewrite it as

$$\frac{\partial n^2}{\partial S_A} = 2n\frac{\partial n}{\partial S_A}. \tag{6}$$

We use the MS equation to calculate n and the partial derivative $\frac{\partial n}{\partial S_A}$ in Eqs. (5) and (6).

To account for pressure in β_T, ρ, and a_0, we followed the approach used by Zhang and Hu (2009b), where β_T, ρ, and a_0 are expressed as functions of the partial derivative of Gibbs energy with respect to temperature, salinity, pressure, or their combinations. Feistel (2008) developed a general equation for specific Gibbs energy of seawater, $g(S_A, T, p)$, over an extended validity range of $0\,\mathrm{g\,kg^{-1}} \le S_A \le 120\,\mathrm{g\,kg^{-1}}$, $-12\,^\circ\mathrm{C} \le T \le 80\,^\circ\mathrm{C}$, and $-0.1\,\mathrm{Pa} \le p \le 100\,\mathrm{MPa}$, where p is sea pressure in Pa, and the absolute pressure $P = 101325 + p$. From thermodynamic statistics (IOC, 2010), we have

$$\rho = \frac{1}{g_p}, \tag{7}$$

$$\beta_T = -\frac{g_{pp}}{g_p}, \tag{8}$$

and

$$\frac{\partial \ln a_0}{\partial S_A} = -\frac{M_w S_A}{RT} g_{ss}, \tag{9}$$

where g_p represents the first-order partial derivative of g with respect to p, and g_{pp} and g_{ss} the second order derivative of g with respect to p and S_A, respectively, and the molar gas constant $R = N_A \times k_B$.

Inserting Eqs. (7) and (8) into Eq. (1) gives

$$\beta_d(90) = \frac{\pi^2 k_B T}{2\lambda^4}\left(\frac{-g_{pp}}{g_p}\right)h_d^2(n), \tag{10}$$

where $h_d(n)$ denotes the right-hand side of Eq. (5). Inserting Eqs. (6), (7) and (9) into Eq. (2) gives

$$\beta_c(90) = \frac{\pi^2 k_B T}{2\lambda^4}\frac{g_p}{g_{ss}}h_c^2(n), \tag{11}$$

where $h_c(n)$ denotes the right-hand side of Eq. (6). Inserting Eqs. (10) and (11) into Eq. (4) gives

$$\beta(90) = \frac{\pi^2 k_B T}{2\lambda^4}\left[\frac{-g_{pp}}{g_p}h_d^2(n) + \frac{g_p}{g_{ss}}h_c^2(n)\right]f(\delta), \tag{12}$$

which can be used to estimate $\beta(90)$ as a function of temperature, salinity, and pressure. In Eq. (12), $\frac{-g_{pp}}{g_p}h_d^2(n)$ represents the fluctuations

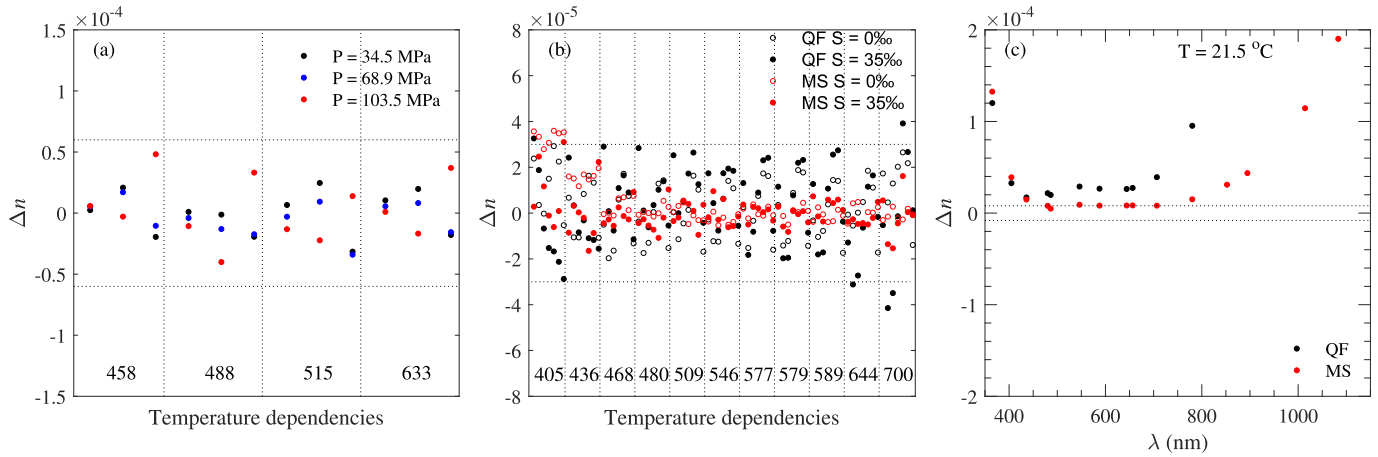

Fig. 1. Differences in the refractive indices of seawater (Δn) calculated using the Millard and Seaver (1990) (MS) equation and those measured by (a) Stanley (1971) for seawater under three different pressures (P), (b) Mehu and Johannin-Gilles (1968) (MG) at two salinities (S) of 0 and 35‰, and at atmospheric pressure, and (c) Daimon and Masumura (2007) (DM) for pure water at temperature $T = 21.5$ °C and at atmospheric pressure. The horizontal dotted lines in (a), (b) and (c) correspond to the quoted experimental uncertainties of 3×10^{-5}, 6×10^{-5}, and 8×10^{-6} for the Stanley, MG, and DM data, respectively. The vertical dotted lines in (a) and (b) separate the sets of data points at each wavelength, and their values are indicated in nanometer at the bottom of the plot. Within a wavelength range, from left to right, the points are for temperatures of 0, 15, and 30 °C in (a) and of 1, 5, 10, 15, 20, 25, and 30 °C in (b). The Quan and Fry (1995) (QF) equation is also compared in (b) and (c).

in the refractive index due to fluctuations in density and $\frac{g_p}{g_{ss}} h_c^2(n)$ represents the fluctuations in the refractive index due to fluctuations in salt concentration (or mixing ratio). The volume scattering function $\beta(\theta)$ at an arbitrary scattering angle θ, total scattering coefficient b, and backscattering coefficient b_b, are as follows:

$$\beta(\theta) = \beta(90)\left(1 + \frac{1-\delta}{1+\delta}\cos^2(\theta)\right), \tag{13}$$

$$b = \frac{8\pi}{3}\beta(90)\frac{2+\delta}{1+\delta}, \tag{14}$$

$$b_b = \frac{4\pi}{3}\beta(90)\frac{2+\delta}{1+\delta}. \tag{15}$$

As there are many terms involved in the Millard and Seaver (1990) equation for the refractive index of seawater and the partial derivatives (McDougall and Barker, 2011) of the Feistel (2008) Gibbs energy equation for seawater, instead of listing the detailed equations here, the MATLAB implementation of our model can be downloaded at: http://tiny.cc/g7wv3y.

3. Results and discussion

We evaluated our model by comparing its results with the measurements conducted at atmospheric pressure by Morel (1966, 1974) for pure water and seawater with a salinity of 38.4‰ at five wavelengths, and those conducted by Cohen and Eisenberg (1965) for pure water at temperatures ranging from 5 to 65 °C and at wavelengths of 436 and 546 nm (Fig. 2). Except for the seawater measurement at 366 nm, the modeled scattering by water agrees with Morel's measurements within the reported experimental uncertainty of 2% (Fig. 2(a)), with median relative difference values of −0.59%, 0.92% and 0.12% for pure water, seawater, and combined comparisons, respectively. Cohen and Eisenberg reported the pure water scattering values normalized to measurements at 25 °C, and modeled values of this ratio agree with the measurements, with median relative differences of 0.41%, −0.62% and 0.08% for 436 nm, 546 nm, and combined comparisons, respectively (Fig. 2(b)).

We do not know why the comparison shown in Fig. 2(a) for seawater at 366 nm is an outlier. The only variable in the model that varies spectrally is the refractive index of water, which affects the scattering by both pure water and seawater. Fig. 1(c) shows that both the MS and QF equations for the refractive index of pure water deviate significantly from the experimental data at 366 nm as compared to the good agreement at visible wavelengths. We can argue that a deviation of similar magnitude should occur for seawater too. However, we estimated that this level of deviation would only result in an error of 0.02% in the modeled scattering, which cannot explain the difference observed in Fig. 2(a). Furthermore, the comparison for pure water at the same wavelength agreed with the measurement well. On the other hand, Morel (1966, 1974) did not mention nor did we find any peculiarity in the seawater scattering measurement at 366 nm.

No measurements were available to evaluate our model at higher pressures. Therefore, we assumed that its performance would be similar to that demonstrated in Fig. 2 under normal conditions, based on the following arguments. First, our model was developed based on the first principles. Therefore, its validity does not depend on the exact pressure values, at least within the range of pressure encountered in the ocean. Second, the model developed in this study and that developed by Zhang et al. (2009) are the same in principle, but differ in their parameterization schemes. Despite this difference, the performance of the two models was similar, and they both compare well with the experimental data (Fig. 2). Therefore, we conclude that the use of different parameterization to account for the effect of pressure does not affect the model's performance. Finally, the model parameterization we adopted in this study was based on the formulae developed and validated for diverse environmental conditions, including the range of pressure encountered in the ocean (Fig. 1(a)).

To understand how light scattering by seawater varies with pressure, we simulated the scattering coefficient by seawater (b_w, m^{-1}) at wavelengths of 400, 532, and 700 nm for a hypothetical situation of constant temperature and salinity of 10 °C and 34 PSU, respectively, from the surface to a depth of 10000 m (Fig. 3). We assumed that the hydrostatic pressure increases by 0.1 MPa for every 10 m increase in depth. For comparison, we also simulated the scattering coefficient by pure water under the same hypothetical situation. Both $\beta_d(90)$ and $\beta_c(90)$ in Eq. (4) decrease with pressure, and, as a result, the total scattering decreases with pressure for both pure water and seawater (Table 1). Increasing pressure suppresses the random motion of molecules, reducing fluctuations in both density and concentration, which in turn cause an overall decrease in scattering by seawater.

The total decrease is greater at shorter wavelengths, where

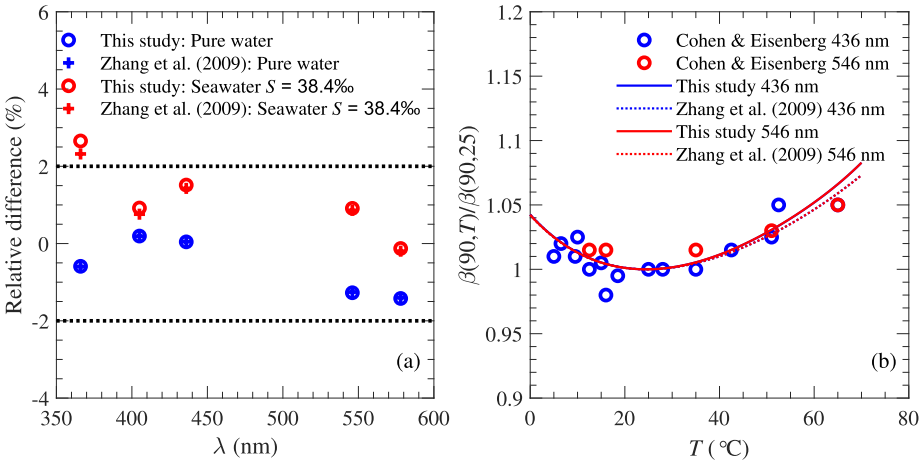

Fig. 2. Evaluation of the seawater scattering model developed in this study and the Zhang et al. (2009) model using published experimental data measured at atmospheric pressure (or zero sea pressure). (a) Relative difference in $\beta(90)$ between the measurements by Morel (1966, 1974) and the modeled values for pure water and seawater with a salinity of 38.4‰ at five wavelengths (λ = 366, 405, 436, 546, and 578 nm) and a temperature of 20 °C. (b) Comparison of pure water $\beta(90)$ normalized to $\beta(90, T = 25\,°C)$ at various temperatures (T) between the measurements by Cohen and Eisenberg (1965) and the modeled values at wavelengths of 436 and 546 nm. Note that the predictions of the Zhang et al. [3] model (blue solid and dotted lines) and that developed in this study (red solid and dotted lines) almost overlap. (For interpretation of the references to color in this figure legend, the reader is referred to the Web version of this article.)

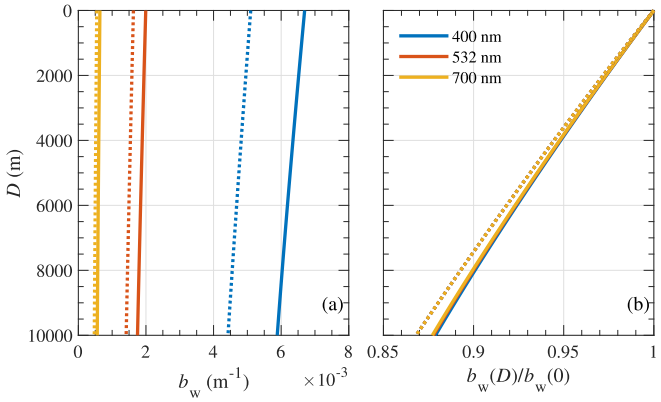

Fig. 3. Absolute (a) and relative (b) changes in the scattering coefficient of water (b_w) calculated using our model as a function of water depth (D) at wavelengths of 400, 532 and 700 nm with a temperature of 10 °C. The solid and dotted lines represent the values for a salinity of 34 PSU and pure water (S = 0 PSU), respectively. In (b), the solid lines overlap, so do dotted lines.

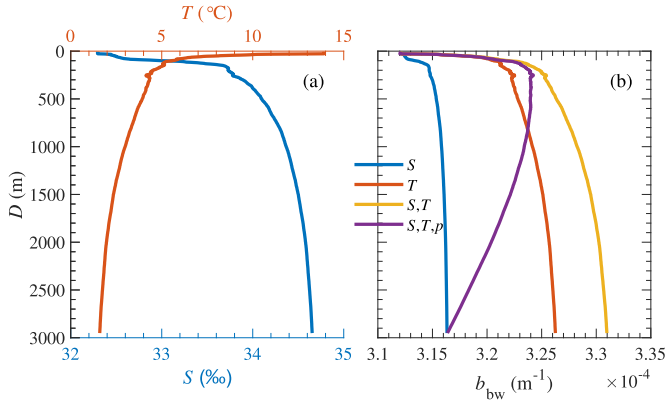

Fig. 4. (a) Variations in temperature and salinity with depth (D) measured on August 25, 2018, near Ocean Station Papa (50° N, 145° W). (b) Backscattering coefficient of seawater (b_{bw}) calculated at 700 nm using the measured CTD data for four scenarios: (1) using measured salinity (S) while assuming invariant temperature and pressure, (2) using measured temperature (T) while assuming invariant salinity and pressure, (3) using measured salinity and temperature (S, T) while assuming invariant pressure, and (4) using measured salinity, temperature, and pressure together (S, T, p). The values for salinity, temperature and pressure that were assumed to be invariant were their respective surface values.

Table 1
$\beta_d(90)$, $\beta_c(90)$ and their sum calculated at 532 nm and at sea pressures (p) of 0, 50 and 100 MPa for pure water and seawater with a salinity of 34 PSU. The values in parentheses indicate the percentage change relative to the surface values.

S (PSU)	p (MPa)	$\beta_d(90)$ (m^{-1}) × 10^{-4}	$\beta_c(90)$ (m^{-1}) × 10^{-4}	$\beta_d(90) + \beta_c(90)$ (m^{-1}) × 10^{-4}
0	0	0.9295	–	0.9295
	50	0.8655 (−6.9%)	–	0.8655 (−6.9%)
	100	0.8086 (−13.0%)	–	0.8086 (−13.0%)
34	0	0.9033	0.3095	1.2128
	50	0.8446 (−6.5%)	0.2901 (−6.3%)	1.1347 (−6.4%)
	100	0.7903 (−12.5%)	0.2742 (−11.4%)	1.0645 (−12.2%)

scattering is stronger (Fig. 3(a)), but the relative change is almost the same, spectrally (Fig. 3(b)). The pressure dependence of scattering varies slightly with salinity, however; from the surface to 10000 m, b_w decreases by approximately 13% and 12% at S = 0 and 34 PSU, respectively (Table 1 and Fig. 3(b)). The small difference in the effect of pressure between pure water and seawater is mainly attributable to the isothermal compressibility term (β_T), which exhibits a greater decrease with pressure in pure water than in seawater (e.g., Safarov et al., 2009).

Knowing that increasing pressure causes a decrease in light scattering by seawater, we examined how scattering changes in the real ocean, where both temperature and salinity, along with pressure, are expected to vary with depth. Fig. 4(a) shows an example of salinity and temperature profiles measured by a CTD cast down to 3000 m on August 25, 2018, near Ocean Station Papa (50° N, 145° W) in the North Pacific Ocean. We calculated the backscattering coefficient (b_{bw}, m^{-1}) at 700 nm for four scenarios to separately examine the effects of salinity, temperature, and pressure. Assuming that temperature and pressure do not vary with depth from their respective values at the surface, an increase in salinity from 32.26 PSU at the surface to 34.65 PSU at 3000 m would cause a 1.4% increase in b_{bw} (blue line in Fig. 4(b)). With similar assumptions about salinity and pressure, a decrease in temperature from 13.93 to 1.59 °C with the same descent would cause an approximately 4.5% increase in b_{bw} (red line in Fig. 4(b)). Note that light scattering by water does not always increase with decreasing temperature. At temperatures of approximately > 28 °C, it increases with temperature (e.g., Fig. 2(b)). Several bulk properties of water (ρ, β_T and n) that affect light scattering all exhibit anomalous patterns with temperature, resulting in a minimum scattering by water that varies from 24.6 °C for pure water to 27.5 °C at 40 PSU (Zhang and Hu, 2018). Assuming a constant pressure, the combined effect of salinity and temperature, as shown in Fig. 4(a), would increase b_{bw} by approximately 6% from the surface to 3000 m (yellow line in Fig. 4(b)).

Accounting for changes in pressure as well as those in salinity and temperature, b_{bw} increased by approximately 4% from the surface to 250 m depth, which roughly corresponded to the bases of both the thermocline and halocline in this particular example. This increase is mainly due to the decrease in temperature and increase in salinity, while the hydrostatic pressure was relatively low. At depths greater than 250 m, the effect of increasing pressure on scattering gradually overcame the effect of the continuous decrease in temperature and continuous increase in salinity, resulting in a net decrease in b_{bw}. At 3000 m, b_{bw} decreased by approximately 3% from its maximum at 250 m. Here, we used the b_{bw} value at 700 nm to illustrate the effect of pressure on scattering by seawater for this particular distribution of temperature and salinity. The exact values of scattering by seawater would differ for different wavelengths or scattering angles, but the relative changes in response to pressure would be similar (Fig. 3(b)).

The Zhang et al. (2009) model, which is widely used (Werdell et al., 2018), does not include the effect of pressure, and therefore only applies to the near-surface water. At depths < 100 m, the seawater scattering values estimated using the Zhang et al. (2009) model and that developed in this study are virtually the same. At greater depths, the pressure effect, if ignored, would lead to the overestimation of molecular scattering. Using the CTD data shown in Fig. 4(a), we estimated that scattering by seawater would be overestimated by 1.5% at 1000 m, and by approximately 4.8% at 3000 m if the effect of pressure were not considered.

Scattering by seawater ($\beta_w(\theta)$) is a background signal that must be subtracted from the bulk scattering measurements ($\beta(\theta)$) to derive the scattering caused by particles ($\beta_p(\theta)$), i.e.,

$$\beta_p(\theta) = \beta(\theta) - \beta_w(\theta). \tag{16}$$

Equation (16) gives,

$$\frac{\Delta\beta_p(\theta)}{\beta_p(\theta)} = \frac{\Delta\beta(\theta)}{\beta(\theta)}\frac{\beta(\theta)}{\beta_p(\theta)} - \frac{\Delta\beta_w(\theta)}{\beta_w(\theta)}\frac{\beta_w(\theta)}{\beta_p(\theta)}, \tag{17}$$

where $\Delta\beta_p/\beta_p$, $\Delta\beta/\beta$, and $\Delta\beta_w/\beta_w$ are the uncertainties in estimating particulate scattering, measuring bulk scattering, and calculating seawater scattering, respectively. One uncertainty in measuring bulk scattering in deeper ocean is associated with Sea-Bird/WETLabs backscatter sensors, for which Poteau et al. (2017) found dark current values obtained in the field often differ from the factory values, with an average difference of 3 counts. While this difference in dark current affects the measurements at all depths, the impact is relatively greater in deeper ocean where particulate backscattering is relatively lower. Assuming that the measurement uncertainty is corrected, i.e., $\Delta\beta/\beta = 0$, the uncertainty in estimating β_p is directly proportional to the uncertainty in calculating β_w, modified by a scaling factor of β_w/β_p.When $\beta_w/\beta_p > 1$, the uncertainties in seawater scattering, while small (Fig. 4(b)), will be amplified and could become a significant source of uncertainty when estimating particulate scattering. This occurs in clear oceanic surface waters (Twardowski et al., 2007) or in mesopelagic regions (Wojtasiewicz et al., 2018), where bulk backscattering is dominated by molecular backscattering by seawater. Fig. 5 illustrates one such example, showing the impact of pressure on estimating particulate backscattering.

Bulk volume scattering functions at 124° ($\beta(124)$) were measured at a wavelength of 700 nm using a Sea-Bird/WETLabs FLBB sensor (S/N FLBBRTD-3522) mounted on a CTD during the NASA EXPORTS 2018 cruise in the North Pacific Ocean onboard the R/V Sally Ride. Three profiles were taken to 3000 m (SR1812-061, SR1812-098, and SR1812-144; Fig. 5(a)). The temperature and salinity profiles among these three casts are almost identical; data from cast SR1812-061 is shown in Fig. 4(a). From measured temperature, salinity, and pressure, we calculated profiles of the volume scattering function due to seawater ($\beta_w(124)$) (solid lines in Fig. 5(b)), accounting for the angular weighting function, which has a full-width-half-maximum (FWHM) spread of 41° for this particular sensor, and a 20 nm bandwidth. For comparison, we also calculated $\beta_w(124, p = 0)$ by assuming a sea pressure of zero, which is currently used when calculating scattering by seawater (dashed lines in Fig. 5(b)). The volume scattering function due to particles, $\beta_p(124)$, is represented by the solid lines in Fig. 5(c). Again, for comparison, we estimated $\beta_p(124)$ using $\beta_w(124, p = 0)$, which is represented by the dashed lines in Fig. 5(c). $\beta_p(124)$ is approximately 60–70% of $\beta_w(124)$ at depths between 1000 and 3000 m, where the pressure reaches 10–30 MPa. If ignored, the effect of pressure on molecular scattering would cause an underestimation of $\beta_p(124)$, as shown by comparison of the dashed and solid lines in Fig. 5(c), with errors ranging from approximately 2–3% at 1000 m to 8–9% at 3000 m.

As another example, Fig. 6 illustrates how pressure affects the estimate of particulate backscattering obtained from a BGC-Argo float that collected measurements from a depth of 2000 m on ascending profiles. The BGC-Argo float (WMO: 5905988, #0949) employed a Sea-Bird/WETLabs MCOMS sensor (SN: MCOMSC-157) to measure the volume scattering function at 150° with a FWHM angle of 20° and at 700 nm with a bandwidth 20 nm. During a recent deployment in the North Pacific Ocean, we estimated that failure to consider the effect of pressure on molecular scattering by seawater resulted in an underestimation of $\beta_p(150)$ by 8–9% at 2000 m and 4–5% at 1000 m (Fig. 6). Fig. 6 suggests, with the developing Deep Argo floats that will be able to obtain measurements to 6000 m (e.g., Jayne et al., 2017), that it is critical to account for the effect of pressure on scattering by seawater.

4. Conclusions

For the first time, we investigated the effect of pressure on light scattering by seawater. We updated the parameterization of the Zhang et al. (2009) model using the Millard and Seaver (1990) equation for the refractive index of seawater and the Feistel (2008) Gibbs function for seawater thermodynamics, both of which were developed as a function of pressure as well as salinity and temperature. Increasing pressure restricts the random thermal motion of water molecules and/or sea salt ions, which leads to a decrease in the microscopic fluctuation of the refractive index of seawater and consequently results in a decrease in light scattering. Our model predicts that molecular scattering by water decreases with water depth, by 12–13% at a depth of 10000 m. If ignored, the effect of pressure on molecular scattering by seawater results in an underestimation in the particulate backscattering from the measurement of bulk backscattering, from which backscattering by seawater needs to be subtracted. The error, however, is negligible in the near-surface waters, such as measurements used in studies related to the satellite remote sensing of ocean color (Werdell et al., 2013). For applications of BGC-Argo floats where direct measurements of backscattering are made at depths to 2000 m, or emerging Deep Argo floats which will profile to depths of 6000 m, the effect of pressure on light scattering by seawater must be considered.

Even though light scattering by liquids and/or solutions has been studied under high pressure (Meier and Kriegs, 2008; Russo et al., 2017), no measurements have been reported for pure water or seawater. Therefore, we cannot validate our model directly. At atmospheric pressure, our model agree with the measurements by Morel (1966) and by Cohen and Eisenberg (1965) with a median difference within ± 1%. Also, further study is required to investigate if and how pressure could affect the depolarization ratio of water, which was assumed to have a constant value of 0.039 in this study.

Acknowledgments

Interest in this work was stimulated by a question from Dr. Emmanuel Boss on the possible effect of pressure on light scattering by water, and was later rekindled by our observations on the pattern of decreasing bulk backscattering at depths greater than 1000 m during the NASA EXPORTS cruise in the North Pacific Ocean in 2018. We

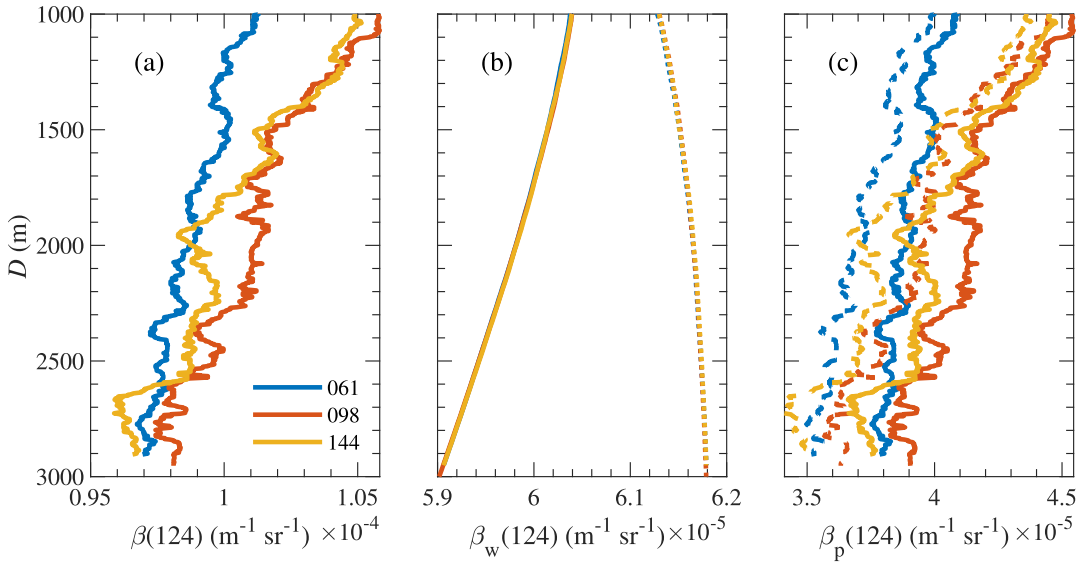

Fig. 5. (a) Bulk volume scattering function measured at a scattering angle of 124° and 700 nm ($\beta(124)$) by a Sea-Bird/WETLabs ECO backscatter sensor (S/N FLBBRTD-3522) in three CTD casts (SR1812-061, −98, and −144) to 3000 m during the NASA EXPORTS 2018 cruise in the North Pacific Ocean. (b) Corresponding volume scattering functions by seawater ($\beta_w(124)$, solid lines) calculated using the measured temperature, salinity, and pressure. Note that the $\beta_w(124)$ values calculated for the three casts were very similar. The dashed lines are the calculated seawater scattering assuming a sea pressure (p) of zero throughout the water column ($\beta_w(124, p = 0)$). (c) Estimated particulate scattering: solid lines = $\beta(124) - \beta_w(124)$; dashed lines = $\beta(124) - \beta_w(124, p = 0)$. Particulate scattering is underestimated when pressure effects are not included.

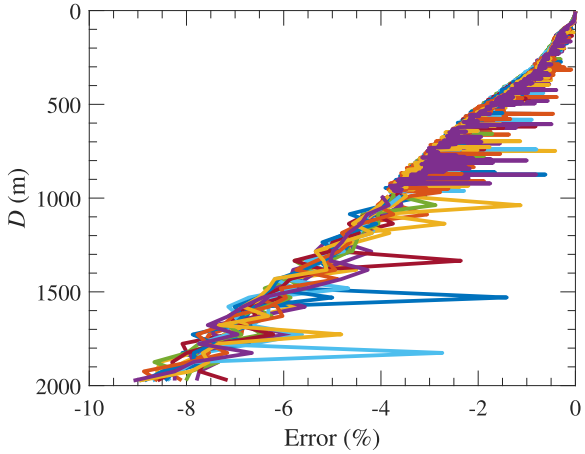

Fig. 6. Underestimation of $\beta_p(150)$ obtained from the BGC-Argo float (WMO: 5905988, #0949) in the recent deployment in the North Pacific Ocean, courtesy of Dr. A. Fassbender. Different colors denote different ascending profiles. (For interpretation of the references to color in this figure legend, the reader is referred to the Web version of this article.)

thank Dr. Andrea Fassbender for providing unpublished data from a BGC-Argo float and Dr. Norm Nelson for assistance in processing the CTD data collected during the EXPORTS experiment. This work was supported by the National Aeronautics and Aerospace Administration (NASA) (NNX15AC85G, 80NSSC17K0656, 80NSSC18M0024, 80NSSC17K0663); National Science Foundation (NSF) (1459168); and National Science Foundation of China (NSFC) (61675187).

Appendix A. Supplementary data

Supplementary data to this article can be found online at https://doi.org/10.1016/j.dsr.2019.03.009.

References

Cabannes, J., 1922. Considérations théoriques sur la diffusion de la lumière par les liquides transparents. Polarisation de la lumière diffusée latéralement. J. Phys. Radium 3 (12), 429–442.
Cohen, G., Eisenberg, H., 1965. Light scattering of water, deuterium oxide, and other pure liquids. J. Chem. Phys. 43 (11), 3881–3887.
Daimon, M., Masumura, A., 2007. Measurement of the refractive index of distilled water from the near-infrared region to the ultraviolet region. Appl. Opt. 46 (18), 3811–3820.
Einstein, A., 1910. Theorie der Opaleszenz von homogenen Flüssigkeiten und Flüssigkeitsgemischen in der Nähe des kritischen Zustandes. Annalen der Physik 338 (16), 1275–1298.
Farinato, R.S., Rowell, R.L., 1976. New values of the light scattering depolarization and anisotropy of water. J. Chem. Phys. 65 (2), 593–595.
Feistel, R., 2008. A Gibbs function for seawater thermodynamics for -6 to 80 °C and salinity up to 120 g kg^{-1}. Deep-Sea Res. I 55, 1639–1671.
IOC, SCOR, IAPSO, 2010. The International Thermodynamic Equation of Seawater – 2010: Calculation and Use of Thermodynamic Properties. UNESCO, pp. 196 (English).
Jayne, S.R., Roemmich, D., Zilberman, N., Riser, S.C., Johnson, K.S., Johnson, G.C., Piotrowicz, S.R., 2017. The Argo program: present and future. Oceanography 30 (2), 18–28.
McDougall, T.J., Barker, P.M., 2011. Getting Started with TEOS-10 and the Gibbs Seawater (GSW) Oceanographic Toolbox. SCOR/IAPSO WG127, pp. 28.
Mehu, A., Johannin-Gilles, A., 1968. Variation de la réfraction spécifique de l'eau de mer étalon de Copenhague et de ses dilutions en fonction de la longuerr d'onde, de la température et de la chlorinité. Cah. Oceanogr. 20, 803–812.
Meier, G., Kriegs, H., 2008. A high pressure cell for dynamic light scattering up to 2kbars with conservation of plane of polarization. Rev. Sci. Instrum. 79 (1), 013102.
Millard, R.C., Seaver, G., 1990. An index of refraction algorithm for seawater over temperature, pressure, salinity, density, and wavelength. Deep Sea Research Part A. Oceanogr. Res. Pap. 37 (12), 1909–1926.
Millero, F.J., Feistel, R., Wright, D.G., McDougall, T.J., 2008. The composition of standard seawater and the definition of the reference-composition salinity scale. Deep Sea Res. Oceanogr. Res. Pap. 55 (1), 50–72.
Morel, A., 1966. Etude Experimentale de la diffusion de la lumiere par l'eau, les solutions de chlorure de sodium et l'eau de mer optiquement pures. Journal de Chimie Physique 10, 1359–1366.
Morel, A., 1974. Optical properties of pure water and pure sea water. In: Jerlov, N.G., Nielsen, E.S. (Eds.), Optical Aspects of Oceanography. Academic Press, New York, pp. 1–24.
Poteau, A., Boss, E., Claustre, H., 2017. Particulate concentration and seasonal dynamics in the mesopelagic ocean based on the backscattering coefficient measured with Biogeochemical-Argo floats. Geophys. Res. Lett. 44 (13), 6933–6939.
Proutiere, A., Megnassan, E., Hucteau, H., 1992. Refractive index and density variations in pure liquids: a new theoretical relation. J. Phys. Chem. 96, 3485–3489.
Quan, X., Fry, E.S., 1995. Empirical equation for the index of refraction of seawater. Appl. Opt. 34 (18), 3477–3480.
Russo, D., Laloni, A., Filabozzi, A., Heyden, M., 2017. Pressure effects on collective density fluctuations in water and protein solutions. Proc. Natl. Acad. Sci. Unit. States Am. 114 (43), 11410–11415.
Safarov, J., Millero, F., Feistel, R., Heintz, A., Hassel, E., 2009. Thermodynamic properties

of standard seawater: extensions to high temperatures and pressures. Ocean Sci. 5 (3), 235–246.
Smoluchowski, M.v., 1908. Molekular-kinetische Theorie der Opaleszenz von Gasen im kritischen Zustande, sowie einiger verwandter Erscheinungen. Annalen der Physik 330 (2), 205–226.
Stanley, E.M., 1971. The refractive index of seawater as a function of temperature, pressure and two wavelengths. Deep Sea Res. Oceanogr. Abstr. 18 (8), 833–840.
Twardowski, M.S., Claustre, H., Freeman, S.A., Stramski, D., Huot, Y., 2007. Optical backscattering properties of the "clearest" natural waters. Biogeosciences 4 (6), 1041–1058.
Werdell, P.J., Franz, B.A., Lefler, J.T., Robinson, W.D., Boss, E., 2013. Retrieving marine inherent optical properties from satellites using temperature and salinity-dependent backscattering by seawater. Opt. Express 21 (26), 32611–32622.
Werdell, P.J., McKinna, L.I.W., Boss, E., Ackleson, S.G., Craig, S.E., Gregg, W.W., Lee, Z., Maritorena, S., Roesler, C.S., Rousseaux, C.S., Stramski, D., Sullivan, J.M., Twardowski, M.S., Tzortziou, M., Zhang, X., 2018. An overview of approaches and challenges for retrieving marine inherent optical properties from ocean color remote sensing. Prog. Oceanogr. 160, 186–212.
Wojtasiewicz, B., Walsh, I.D., Antoine, D., Slawinski, D., Hardman-Mountford, N.J., 2018. Inferring and removing a spurious response in the optical backscattering signal from an autonomous profiling float. J. Atmos. Ocean. Technol. 35 (11), 2137–2146.
Zhang, X., Hu, L., 2009a. Estimating scattering of pure water from density fluctuation of the refractive index. Opt. Express 17 (3), 1671–1678.
Zhang, X., Hu, L., 2009b. Scattering by pure seawater at high salinity. Opt . Express 17 (15), 12685–12691.
Zhang, X., Hu, L., 2018. Anomalous light scattering by pure seawater. Appl. Sci. 8 (12), 2679.
Zhang, X., Hu, L., He, M.-X., 2009. Scattering by pure seawater: effect of salinity. Opt. Express 17 (7), 5698–5710.